Industrial Chemistry & Materials

ROYAL SOCIETY OF CHEMISTRY

MINI REVIEW

View Article Online
View Journal | View Issue

Cite this: *Ind. Chem. Mater.*, 2023, **1**, 299

Designing active and stable Ir-based catalysts for the acidic oxygen evolution reaction

Zijie Lin, Tanyuan Wang * and Qing Li *

The widespread application of polymer electrolyte membrane water electrolyzers (PEMWEs) remains a tough challenge to date, as they rely on the use of highly scarce iridium (Ir) with insufficient catalytic performance for the oxygen evolution reaction (OER). Therefore, exploring the degradation and activation mechanism of Ir-based catalysts during the OER and searching for highly efficient Ir-based catalysts are essential to achieve large-scale hydrogen production with PEMWEs. This minireview briefly describes the adsorbate evolution mechanism and lattice oxygen oxidation mechanism for Ir-based catalysts to complete the OER process. Then, the valence change of Ir during the OER is discussed to illustrate the origin of the favorable stability of Ir-based catalysts. After that, different modification strategies for IrO_2, such as elemental doping, surface engineering, atom utilization enhancing, and support engineering, are summarized in the hopes of finding some commonalities for improving performance. Finally, the perspectives for the development of Ir-based OER catalysts in PEMWEs are presented.

Keywords: Polymer electrolyte membrane water electrolyzers; Oxygen evolution reaction; Iridium catalysts; Degradation mechanism; Hydrogen production.

Received 29th June 2023,
Accepted 24th July 2023

DOI: 10.1039/d3im00070b

rsc.li/icm

1 Introduction

With the growth of global population and environmental concern, it is desperately required to develop renewable energy technologies. Green hydrogen is considered as one of the most promising choices to achieve the target of being carbon-neutral due to the zero environmental impact of its production.[1–3] Electrochemical water splitting (EWS) technologies, which can directly convert electrical energy into chemical energy, show great potential for hydrogen generation. Currently, low temperature EWS technologies can be divided into three categories, alkaline water electrolyzers (AWEs), anion exchange membrane electrolyzers (AEMWEs) and PEMWEs.[4–6] Conventional AWEs have enabled large-scale hydrogen production due to their low cost. However, their high energy consumption and low hydrogen purity limit their development. Currently, AEMWEs and PEMWEs have been proposed to improve the working current density and hydrogen production efficiency.[4] AEMWEs mainly utilize non-precious metal materials with low catalyst costs, but their hydrogen production efficiency still needs to be further

State Key Laboratory of Materials Processing and Die & Mould Technology, School of Materials Science and Engineering, Huazhong University of Science and Technology, Wuhan, Hubei 430074, China. E-mail: wangty@hust.edu.cn, qing_li@hust.edu.cn

Zijie Lin

Zijie Lin is currently pursuing his Ph.D. in materials science at Huazhong University of Science and Technology under the supervision of Prof. Qing Li. He received his B.S. in materials science at Lanzhou University in 2020. His research interest focuses on durable electrocatalysis for the oxygen evolution reaction and oxygen reduction reaction.

Tanyuan Wang

Tanyuan Wang is currently an associate professor at the School of Materials Science and Engineering in Huazhong University of Science and Technology (HUST), China. He received his PhD in Chemistry from Peking University in 2015 and worked as a visiting scholar at Stanford University from 2017 to 2018. His current research is focused on electrocatalysis and nanomaterials synthesis.

improved due to their low OH^- conductivity in an alkaline environment. On the other hand, the PEMWE technologies have attracted increasing attention owing to their high proton conductivity (0.1 ± 0.02 S cm^{-1}) in proton exchange membranes, terrific conversion efficiency,[6] and relatively high hydrogen purity, which makes it a promising hydrogen production technology. However, large-scale application of this technology is severely hindered by the high cost and limited activity/durability of the catalysts, especially on the anode.[7–9]

The anodic oxygen evolution reaction (OER) plays a significant role in the development of efficient PEMWEs.[10] Since the 1950s, many studies on the OER mechanism of various metals have been conducted.[7] Among the materials, Ir-based catalysts have been demonstrated to be good candidates for the application in water electrolysis due to their relatively high activity and stability under high voltage (>1.6 V) and harsh acidic (pH < 1) working conditions in PEMWEs.[11–13] However, high loading (>0.5 mg_{Ir} cm^{-1}) of costly Ir (~US$60 670 per kg) is required for practical devices.[14] Moreover, the activity of current commercial Ir catalysts also needs to be further improved to achieve high energy conversion efficiency at large current density (*e.g.*, 2025 US Department of Energy (DOE) target, <1.9 V@3 A cm^{-2}).[15] Besides, Ir-based catalysts still face an inevitable dissolution problem at a potential higher than 1.4 V.[16] Therefore, tremendous effort has been put into investigating the activation and dissolution mechanisms of Ir, so as to develop low-cost and efficient Ir-based OER catalysts.

In this review, we first introduce the activation and degradation mechanism of Ir-based catalysts. Then, various strategies for the optimization of Ir-based OER catalysts are summarized, including modification of electronic structure by elemental doping, achieving corrosion resistance through surface engineering, improving atomic utilization by reducing particle size or atomization and enhancing electron interactions through support engineering. Finally, some perspectives on the design of cost-effective Ir-based catalysts have been presented. We hope that these can help develop Ir-based catalysts with high OER activity and stability under the operating conditions of PEMWEs, and benefit large-scale hydrogen production from renewable clean energy sources.

Qing Li

Qing Li is a professor at the School of Materials Science and Engineering in Huazhong University of Science and Technology (HUST), China. He received his PhD in Chemistry from Peking University in 2010 and then worked as a postdoctoral research associate at Los Alamos National Laboratory (2011–2013) and Brown University (2013–2015). His current research interests focus on developing advanced electrocatalysts and devices for fuel cells and electrolysis.

2 OER mechanism of Ir-based catalysts

The OER is a complicated electrochemical reaction involving several reaction pathways and oxygen intermediates. According to the conventional adsorbate evolution mechanism (AEM), surface metal atoms or ions act as the active sites on which H_2O molecules go through the transfer process of four protons and electrons to generate oxygen intermediates and finally O_2.[17] The most significant feature is that oxygen is firmly restricted to the lattice and does not participate directly in the reaction. Most of the materials reported to date accomplish the OER mainly through this mechanism.[18,19] For example, Hong *et al.*[20] reported that Ir–NiFeO followed the AEM to complete the OER because the Ni–O–Fe bridge structure facilitated the immobilization of lattice oxygen. More recently, an alternative pathway, which involves a direct $*O–O_{lattice}$ bond coupling, has been identified as a lattice oxygen oxidation mechanism (LOM) in the OER. As shown in Fig. 1a, the LOM can bypass the generation of *OOH in the AEM (step 3) and couple the lattice oxygen of materials to directly generate oxygen (step 5). Wang *et al.*[21] reported that the high OER activity of Ir/CoNiB was intrinsically dominated by the LOM pathway instead of the AEM, which was triggered by the formation of an Ir–O–Co bridge and activation of lattice oxygen. The interaction of the metal cation with the oxygen anion orbital is correlated with the OER mechanism. It is indicated that when the p-band center of the oxygen atom is close to the Fermi energy level of the metal oxide, the covalency of the metal with oxygen is enhanced to trigger the excitation of the lattice oxygen, thus following the LOM (Fig. 1b). Therefore, enhancing the orbital coverage of Ir and O will be an option for the better involvement of lattice oxygen in the reaction. Despite the promise of lower OER overpotential, the stability of metal oxides based on the LOM remains challenging. In the LOM pathway, the continuous formation of oxygen vacancies and dissolution of cations during lattice oxygen redox can lead to extensive oxygen diffusion and structural collapse.[22,23] Therefore, a reliable approach for the design of high-performance OER catalysts is provided by balancing the highly stable AEM with the highly active LOM pathway.[24] For example, Xi *et al.*[25] realized the arbitrarily transformed AEM–LOM–AEM to achieve the co-optimization of activity and stability by modifying the oxygen defect contents in $La_xSr_{1-x}CoO_{3-\delta}$ catalysts, which offered an inspiring strategy to coordinate the activity and stability of the catalysts in the OER by the regulation of reaction mechanisms.

Although Ir catalysts can efficiently adsorb oxygen intermediates during the OER, Ir still undergoes oxidative dissolution at high potentials ($E > 1.4$ V_{RHE}) according to the

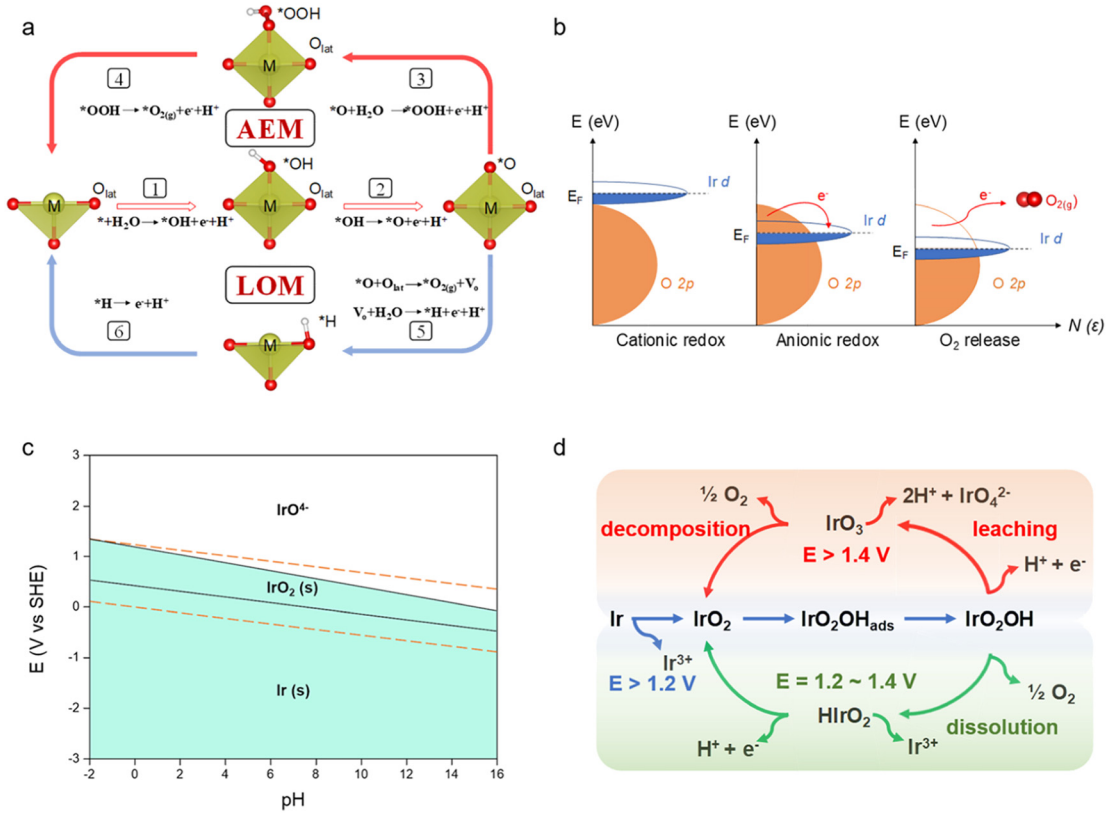

Fig. 1 (a) Schematic representation of the adsorbate evolving mechanism (AEM) and lattice oxygen mechanism (LOM); the four electrochemical reaction steps for each mechanism are shown with "*" and V_O denotes the lattice oxygen vacancy, respectively. M stands for the metal (Ir); (b) schematic representation of the energy level *versus* density of states N(ε); (c) pH–potential diagram of Ir. (d) Universal mechanism for Ir catalysts correlating both the OER and dissolution pathways.

Pourbaix program (Fig. 1c). On the other hand, the formation of active oxygen intermediates depends on the oxidation state of iridium.[26–28] When the catalyst is electrochemically processed at high potentials, positive charges can be accumulated on electron-deficient oxygen due to the strong orbital hybridization of oxygen and oxidized iridium, which benefits the OER by decreasing the activation energy for nucleophilic attack of water molecules and O–O bond formation.[7] Therefore, it is necessary to understand the valence change of the Ir-based catalysts and suppress their over-oxidation. The dissolution of Ir can be correlated into a universal scheme (Fig. 1d).[9] Generally, Ir would be oxidized to IrO_2 during the OER, followed by the adsorption of *OH ("*" stands for radical) on the surface of IrO_2. Then, the Ir center is further oxidized, which leads to the formation of the IrO_2(OH) intermediate (outlined in Fig. 1d with blue arrows).[29] Subsequently, IrO_2(OH) can be oxidized to IrO_3 at a potential higher than 1.4 V. And IrO_3 will decompose to O_2 and IrO_2 to close the reaction loop or react with water to form dissolved IrO_4^{2-} (outlined in Fig. 1d with red arrows).[30] And this competition is affected by the different rates for hydrolysis and decomposition, which is determined by the electronic structure, crystalline surface and coordination environment of various IrO_2. Meanwhile, when the potential is relatively low (E = 1.2–1.4 V_{RHE}), IrO_2(OH) may decompose to O_2 and form $HIrO_2$ intermediates. And $HIrO_2$ intermediates will be further oxidized to IrO_2 or dissolve as Ir^{3+} (outlined in Fig. 1d with green arrows). Studies have shown that when $HIrO_2$ has fast dissolution kinetics, dissolution in the form of Ir^{3+} is the main pathway for its performance decay. If its structure is stable enough, redeposition back to IrO_2 is more likely to occur under the applied potential.[31] Besides, metallic Ir would also be oxidized to Ir^{3+}, thus leading to degradation of the catalysts.

The understanding of the OER and dissolution mechanism can provide insights into the structure–performance relationship of Ir-based materials. The adsorption/desorption ability of oxygen species for Ir-based catalysts is the most critical factor for the performance of the OER. In order to improve the activity and stability of a catalyst, the oxygen intermediate binding energy of the active center should be optimized. Moreover, the valence state of Ir should be monitored to inhibit its degradation. Considering the above mechanism, several strategies such as elemental doping, surface engineering, atom utilization enhancing, and support engineering are carried out to achieve high activity and stability in either the AEM or the LOM for Ir-based catalysts. Following with these modification strategies, we try to disclose the activation and the degradation mechanism of Ir-based catalysts as well as provide guidelines for the design of efficient Ir-based catalysts.

3 Strategies for improving the OER performance of Ir-based catalysts

3.1 Heteroatom doping

In order to reduce the loading of Ir and improve its utilization, heteroatoms are doped into Ir to form alloys. According to the principles of physical chemistry, the catalytic activity and stability of an alloy are closely related to its crystalline structure. The bond length and the atomic coordination environment would affect the electronic structure of the active sites, thus regulating the binding energy between the active sites and the oxygen-containing intermediate. An Au@$AuIr_2$ core–shell structure was synthesized to balance the binding energies of different intermediates, which displayed 5.6 times higher mass activity than a commercial Ir catalyst for the OER.[32] However, IrM alloys with disordered atomic arrangements are susceptible to metal dissolution at high voltages and in acidic environments, leading to the destruction of the catalyst structure.[33] Specifically, intermetallic compounds may have activity and stability superior to disordered alloys.[34–37] These merits are attributed to the more negative structure formation energy and stronger d–d orbital coupling of intermetallic nanocrystals, which greatly enhance the vacancy formation energy and corrosion-resistance of transition metals in acidic environments.[38] For example, the B2-IrGa intermetallic alloy adopts ordered atomic donor–acceptor architectures.[39] The electron-rich Ir sites in the body-centered cubic (bcc) structure facilitate electron transfer between the Ir atoms and the adsorbed species, effectively lowering the energy barrier for the rate-determining step in the OER (Fig. 2a–e). Moreover, forming Ir into an ordered intermetallic phase with low electronegative Ga will create an electron-rich environment for Ir atoms and enhance the strength of Ir–Ga to suppress the oxidative dissolution and improve the stability of the IrGa catalysts.

Meanwhile, the surface of the Ir alloy will be oxidized during the OER process to form the core@shell structure of Ir alloy@IrO_x.[40] Therefore, direct elemental doping of IrO_2 may seem to be a more effective method to achieve performance tuning. Elemental doping can optimize the d-band center of Ir or the p-band center of O, thus modulating the adsorption energy of the active center for oxygen intermediates.[41] It may also introduce valence change and surface strain due to the inconsistent ionic valence and radius of other elements compared with Ir, which leads to the change in OER performance.[42] An Ag_1/IrO_x catalyst with Ag single atoms embedded in IrO_2 is suggested to activate the surrounding Ir atoms by promoting their valence state (Ir^{x+}, $x > 4$), thus optimizing the adsorption for oxygen intermediates and displaying a low overpotential of 224 mV at 10 mA cm^{-2} and a long-term stability better than commercial catalysts Ir/C.[43] Further, the doping of stable high-valence elements such as W with IrO_x can effectively suppress the dissolution of Ir at ~1.6 V. He *et al.* synthesized a ternary $Ir_{0.7}W_{0.2}Sn_{0.1}O_x$ catalyst to achieve a robust durability of over 220 h at 1 A cm^{-2} in H_2SO_4.[44] The co-

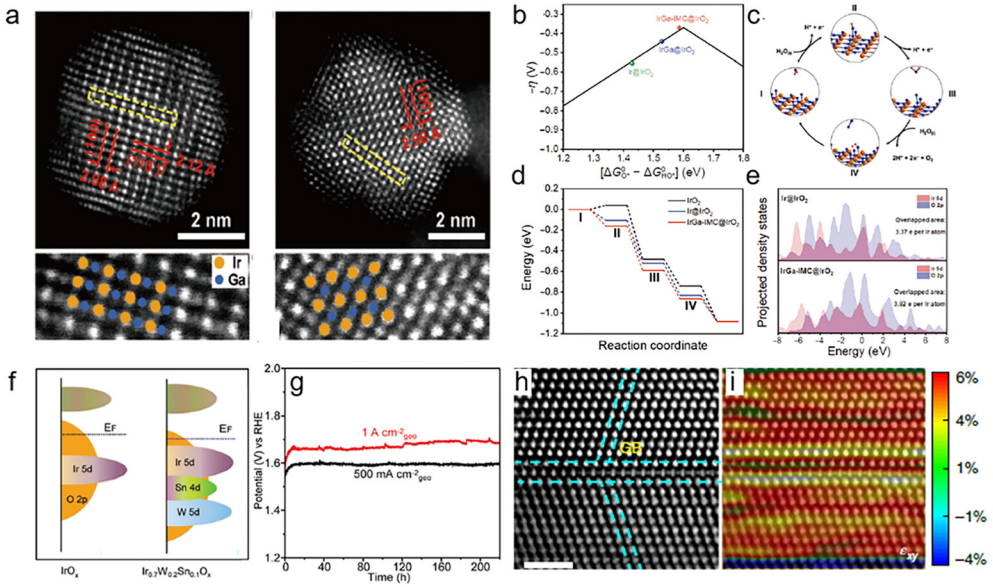

Fig. 2 (a) Aberration-corrected HAADF-STEM images and magnified HAADF-STEM images of IrGa-IMC, with the overlapping schematics of the Ir/Ga atoms; (b) the negative theoretical overpotential was plotted against the standard free energy of the $[\Delta G^0_{O*}-\Delta G^0_{OH*}]$ step; (c) schematic illustration of the OER process on the IrO_x surface in acidic electrolytes; (d) energy profiles of the OER on IrGa-IMC@IrO_2 (red line), Ir@IrO_2 (blue line), and IrO_2 (black line) substrates at U = 1.53 eV *vs.* NHE; the label (I)–(IV) mean the adsorption of H_2O, intermediate OH*, O*, OOH*, respectively. (e) Projected densities of states (pDOS) of Ir@IrO_2 (upper) and IrGa-IMC@IrO_2 (lower), showing the overlapped states of Ir 5d (red) and O 2p (blue) (reproduced with permission from ref. 39, Copyright (2021) Tsinghua University Press and Springer-Verlag GmbH Germany); (f) schematic diagrams of the band structures for IrO_x and $Ir_{0.7}W_{0.2}Sn_{0.1}O_x$; (g) chronopotentiometry curves for $Ir_{0.7}W_{0.2}Sn_{0.1}O_x$ at 500 mA cm^{-2}_{geo} and 1 A cm^{-2}_{geo} (reproduced with permission from ref. 44, Copyright (2022) Wiley-VCH GmbH); the corresponding GPA images for axial strain (ε_{xx}) (h) and shear strain (ε_{xy}) (i) analyses (reproduced with permission from ref. 47, Copyright (2021) Springer Nature).

doping of W and Sn efficiently stabilizes the valence state of Ir through multistage charge redistribution (Fig. 2f–g). In addition, the compressive strain introduced by the elemental doping causes a downward shift of the d-band center of Ir, which will decrease the adsorption energy of *O intermediate on Ir active site.[45] In general, IrO_2 with compressive strain may have better OER performance because the adsorption of oxygenated intermediates on IrO_2 the adsorption energy of oxygenated intermediate on pure IrO_2 is slightly higher than the optimal value.[46] The torsion-strained $Ta_{0.1}Tm_{0.1}Ir_{0.8}O_x$ catalyst exhibits a low overpotential of 198 mV at 10 mA cm^{-2} in H_2SO_4 and operates stably at 1.5 A cm^{-2} for 500 hours in electrolyzers, which is ascribed to the maintained valence state and strain effects caused by the doping (Fig. 2h–i).[47]

Generally, after elemental doping, the electronic structure of Ir and the adsorption or desorption energy of oxygen species can be optimized, thus demonstrating enhanced OER activity. Moreover, the elemental doping can induce strong hybridization between Ir 5d and O 2p, thus inhibiting the excessive oxidation of Ir and the dissolution of Ir, as well as the detachment of oxygen. Meanwhile, the cost of the catalyst can be effectively reduced by the addition of non-precious metal M. Therefore, doping is suggested to be the most

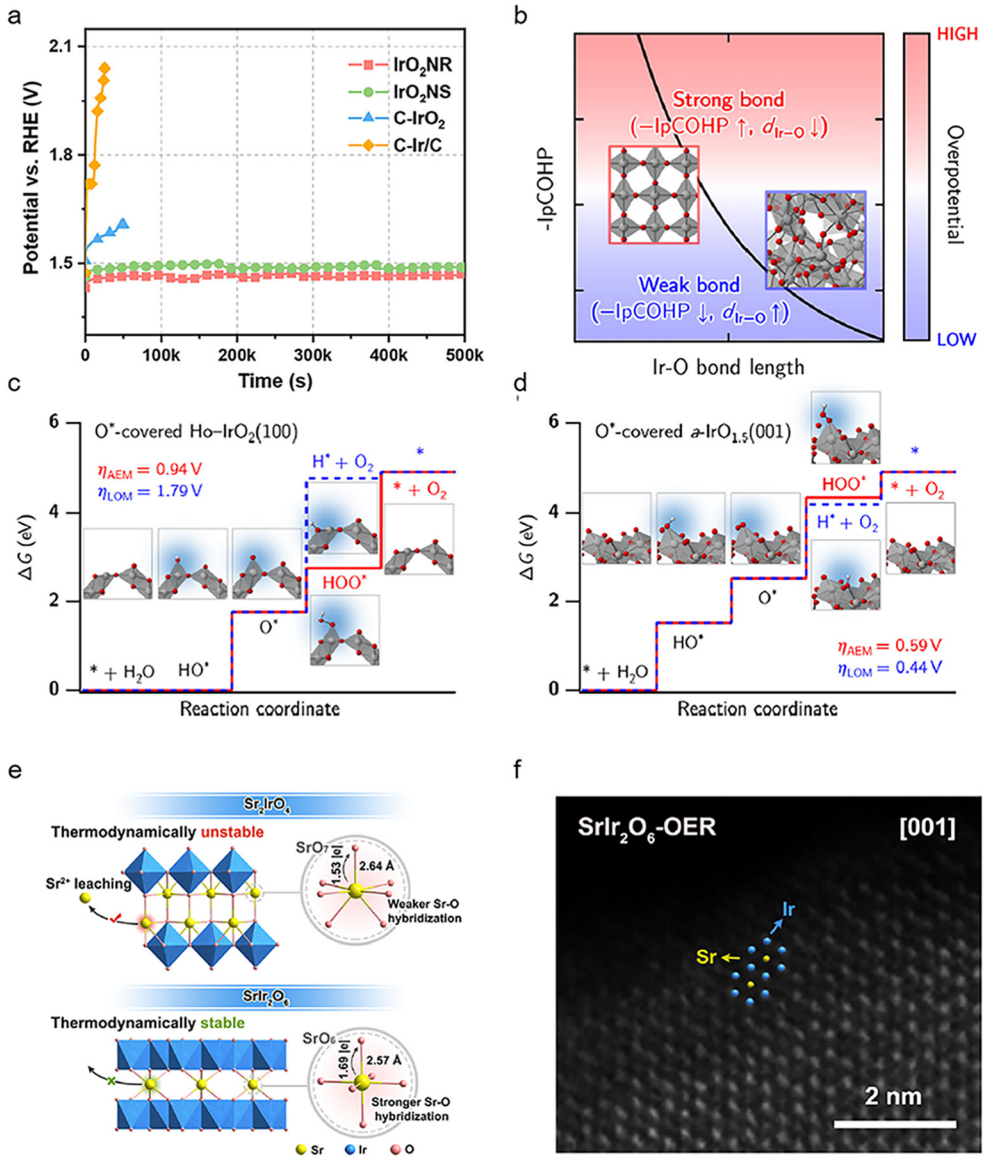

Fig. 3 (a) Chronopotentiometry curves of the IrO_2NR, IrO_2NS, C–IrO_2 and C–Ir/C samples at a constant current density of 10 mA cm^{-2} (reproduced with permission from ref. 48, Copyright (2023) Springer Nature); (b) schematic view of the empirical relationship between Ir–O bond length, –IpCOHP, and overpotential. The iridium and oxygen atoms are depicted as gray and red spheres, respectively, while the IrO_6 octahedra is shaded in gray; (c) O*-covered H_o-IrO_2(100) and (d) O*-covered a-$IrO_{1.5}$(001). The corresponding atomic structures for each reaction step are also provided alongside the ΔG diagrams. The iridium, oxygen, and hydrogen atoms are depicted as gray, red, and white spheres, respectively (reproduced with permission from ref. 53, Copyright (2022) Springer Nature); (e) schematic showing the key factors controlling the structural stability of $SrIr_2O_6$ and Sr_2IrO_4; (f) special aberration-corrected HAADF-STEM image of $SrIr_2O_6$-OER (reproduced with permission from ref. 18, Copyright (2023) American Chemical Society).

promising strategy for designing high performance Ir-based OER catalysts for PEM electrolyzers.

3.2 Surface engineering

The exposed surfaces of the Ir catalysts directly affect their activity and stability for the OER since the surface atoms are the real reaction sites for the adsorption/desorption of reactive oxygen species. A common method to adjust the exposed surface of IrO_2 is to change its crystalline phase. Recently, it is found that the monoclinic phase IrO_2 has a more suitable oxygen intermediate adsorption energy and higher activity compared to the rutile phase counterpart, which is mainly attributed to the exposed crystallographic surface of the monoclinic phase IrO_2 (100) surface.[48] In addition to the most closely packed surface, sufficient utilization of the high-index crystal surfaces has attracted increasing attention.[49] High-index crystalline surfaces may contain a high density of step atoms, which have a low coordination number and high chemical activity and can easily interact with reactant molecules to break chemical bonds and become catalytically active centers. For example, IrO_x with high index planes formed from concave Ir surfaces during the OER exhibits ~10 times higher activity than the Ir (100) planes in acidic OER catalysis (Fig. 3a).[50]

Compared with crystalline IrO_2, an amorphous IrO_x surface may require a lower energy barrier to form the active IrO_3,[51] thus improving the kinetics of the OER. The high surface flexibility and involvement of amorphous IrO_x lattice oxygen facilitate the interaction of adsorbed species between adjacent surface sites.[52] According to the recent reports, amorphous IrO_2 surface can just require an overpotential of about 0.20 V to complete the OER because of the presence of flexible atomic charges and the activation/stretching of the Ir–O bond, while for crystalline IrO_2 the overpotential is 0.4 V.[53] The relatively long Ir–O bond length and weak Ir–O bond strength in amorphous iridium oxides benefit their LOM pathway with a lower theoretical OER overpotential, while the crystalline IrO_2 can only complete the OER through the AEM (Fig. 3b–d). However, amorphous IrO_x will suffer from dissolution to generate more leachable IrO_4^{2-} due to the higher surface flexibility and relatively weak Ir–O interaction caused by the unsaturated coordination of amorphous IrO_x, leading to high activity and low stability. More recently, Zou *et al.*[18] found that the honeycomb layered strontium iridate ($SrIr_2O_6$) retained its crystallinity after the OER and avoided the formation of an amorphous IrO_x layer on the surface, which exhibited high stability (Fig. 3e and f). The enhanced crystallinity in IrO_x will benefit the transformation from IrO_3 into IrO_2 and alleviate the Ir leaching, which is probably ascribed to the faster decomposition kinetics from IrO_3 to IrO_2 than that of hydrolysis/dissolution. Therefore, in order to obtain OER catalysts with high activity as well as high stability, it is necessary to investigate the electronic structure of IrO_2 with various crystallinities as well as their structural changes during the OER process.

3.3 Atom utilization enhancement

In the actual catalytic environment, only a few layers of atoms on the surface are involved in the catalytic reaction as active sites. Hence, in addition to the adjustment of the exposed surface, the particle size of Ir-based materials is also a key issue since it would affect the specific surface area of the material and the number of exposed active sites. When the particle size decreases, atomic utilization and mass activity generally increase.[54] As previously reported, IrO_2 particles with sizes of less than 10 nm could be synthesized by a silica coating method.[55] Compared to commercial IrO_2 (~30 nm), the IrO_2 treated at 800 °C (~7.4 nm) exhibits 1.65-fold higher mass activity at 1.5 V_{RHE}, while the mass activity of 400 °C heat-treated IrO_2 (~3.5 nm) is up to 40 times higher. However, the stability of the 400 °C heat-treated IrO_2 is worse than that of the 800 °C-treated IrO_2, which is due to its poor crystallinity and the involvement of lattice oxygen (Fig. 4a and b). Moreover, in order to further mitigate the high cost of Ir, atomization of the Ir active sites is employed to improve their metal utilization. For example, the as-developed Ir single atom catalyst (SAC) exhibits much higher turnover frequency (24.3 e per site per s at 0.85 V_{RHE}) and mass activity (12.2 A mg_{Ir}^{-1}) than the commercial Ir nanoparticles.[56] Therefore, uniform Ir SACs with great atom-utilization efficiency have received wide interest in recent years.[57] As the size of Ir reaches the cluster or single-atom level, its electronic structure properties and atomic coordination environment would change significantly compared to IrO_2 particles. The atomically dispersed Ir SACs usually exhibit a unique electronic structure due to the distinctive coordinated environments, metal–support interactions, and quantum size impact. For example, Ir single atoms are prone to transfer electrons when in contact with other heteroatoms due to the different electronegativity, and thus the valence state of Ir active centers can be controlled and the adsorption behavior for intermediates can be optimized. Ir–$NiCo_2O_4$ with single-atom Ir sites can display a low overpotential of 240 mV at 10 mA cm^{-2} and long-term stability of 70 h in acidic media, which originates from the electron transfer between the atomic Ir and $NiCo_2O_4$ surface.[58] The interaction between Ir and Co sites can alleviate the over-oxidation of the Ir to enhance the stability of the electrocatalyst (Fig. 4c). Moreover, it has been reported that the strength of the bond between atomically dispersed Ir SACs and the substrate can be regulated to activate lattice oxygen and trigger the LOM. Ge *et al.*[24] presented an effective way to regulate the bond covalency to activate lattice oxygen and LOM through the introduction of Ir single sites to MnO_2 (Fig. 4d). Due to the local doping of Ir single atoms, the whole crystal structure will not be damaged when the lattice oxygen is involved in the reaction. Therefore, Ir–MnO_2 presents a promising low overpotential of 218 mV at 10 mA cm^{-2} and a stable response in the 650 h durability test.

The rational development of single-atom Ir catalysts can effectively modulate the electronic structure of Ir and realize

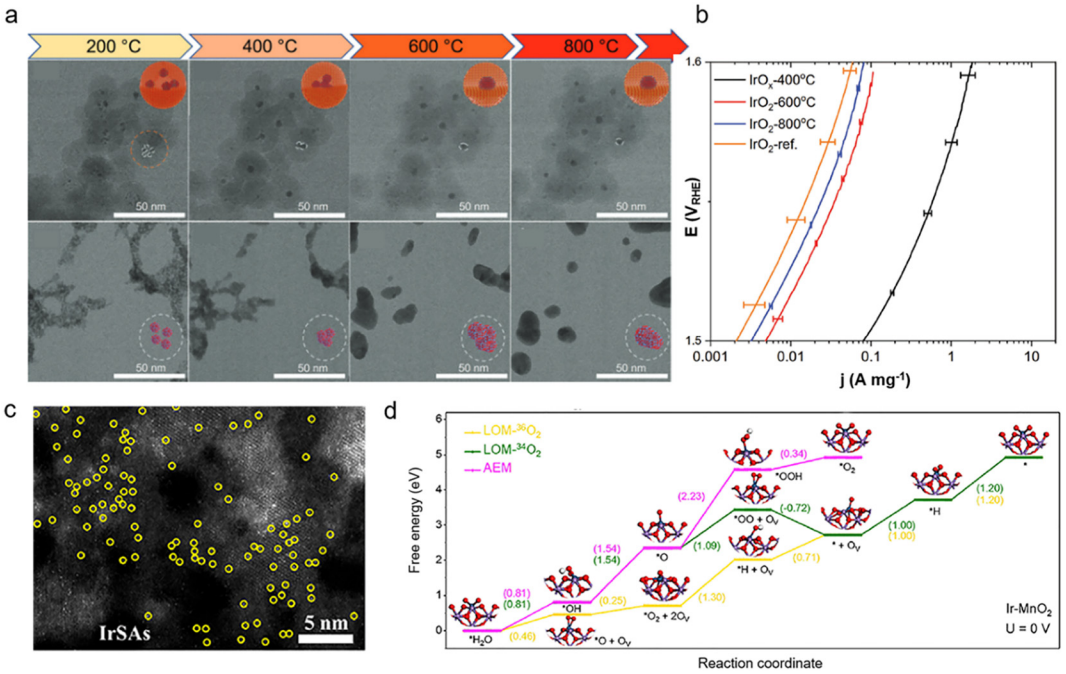

Fig. 4 (a) Structural evolution comparison between silica encapsulated (IrO_x@SiO_2) and bare iridium oxide nanoparticles during the *in situ* heating STEM experiment. Selected STEM snapshots of IrO_x@SiO_2 and bare iridium oxide nanoparticles were taken during the *in situ* consecutive heat treatment in an oxygen atmosphere at 200, 400, 600, and 800 °C; (b) mass normalized activities obtained from first linear sweep voltammetry (LSV) (*iR*-corrected) scanning between 1.3 and 1.6 V_{RHE} (reproduced with permission from ref. 55, Copyright (2023) Wiley-VCH GmbH); (c) HAADF-STEM image of Ir–$NiCo_2O_4$ NSs, showing the Ir-SAs (reproduced with permission from ref. 58, Copyright (2020) American Chemical Society); (d) Gibbs free energy diagrams for the OER on the Ir–MnO_2 (100) surface at 0 V based on the AEM and LOM (reproduced with permission from ref. 24, Copyright (2021) Elsevier Inc.).

the mechanism transition (*e.g.* from the AEM to the LOM) by tuning the strength and binding energy of Ir–O. At higher current densities (*e.g.* >100 mA cm^{-2}), the SACs require higher overpotentials to complete the OER due to their inability to accommodate multiple sites in contact with the intermediates for the simultaneous release of the oxygen species, resulting in lower kinetic rates. Meanwhile, the individual sites tend to dissolve or agglomerate at high potentials, resulting in a decrease of the catalysts' active sites or a change in their electronic structure, which in turn exacerbates the decay of their activity and stability.[59,60] Therefore, single-atom Ir catalysts still need to be further optimized for practical application.

3.4 Engineering catalyst–support interactions

The electronic structure and performance of Ir-based catalysts can also be modified by adjusting the intrinsic interaction between the catalysts and the supports.[61] Carbon-based materials are often used as supports for electrocatalysts. However, carbon will undergo serious corrosion under the operating voltage of the OER, which makes it unsuitable as a support for Ir-based catalysts.[62] According to the pH–potential diagrams, some oxides with strong binding energy, such as SnO_2 *etc.*, can be stable electrocatalyst supports with strong anti-corrosion resistance under the conditions of strong acid and high voltage. Even though the conductivity of the oxide support is generally low, it can be improved through structural modulation such as the doping of metal ions with different valence states and the incorporation of extrinsic conductive supports. These methods will contribute to the accelerated electron transfer as well as the optimization of the adsorption/desorption energy for the intermediates.[63] Recently, the effects of conductivity (determined by the doping level) of the SnO_2 support as well as the Ir loading for Ir–SnO_2 on OER activities were investigated.[64] Sb-doped SnO_2 (ATO) can reach a high conductivity of 3.6 S cm^{-1}, and Ir-ATO with 25% Ir loading achieves a current density of 63 A g_{Ir}^{-1} at an overpotential of 300 mV, exceeding that of commercial TiO_2-supported IrO_2 (Fig. 5a). Meanwhile, the intrinsic electronic metal–support interaction (EMSI) between oxide supports and Ir catalysts can effectively inhibit the oxidative dissolution of Ir.[65] And this interaction can increase the binding energy and migration barrier for Ir atoms, leading to the high electrocatalytic stability of the catalysts. Moreover, the electrocatalyst support can modulate the d-band structure of Ir through lattice strain and electron transfer, thus optimizing the adsorption free energy of oxygen-containing intermediates (*OH, *OOH, *O) and enhancing the OER activity. For example, the Ir:WO_3/Ir catalyst achieves a high mass activity of 13.8 A mg_{Ir}^{-1} at 10 mA cm^{-2} in 0.5 M H_2SO_4 with 32 days of stable response, which originates from the stabilization of high-valence Ir sites with optimized binding energies to oxygen species (Fig. 5b).[66] Recently, Xing *et al.*[15] reported that the Nb_2O_{5-x} loaded Ir catalysts, which

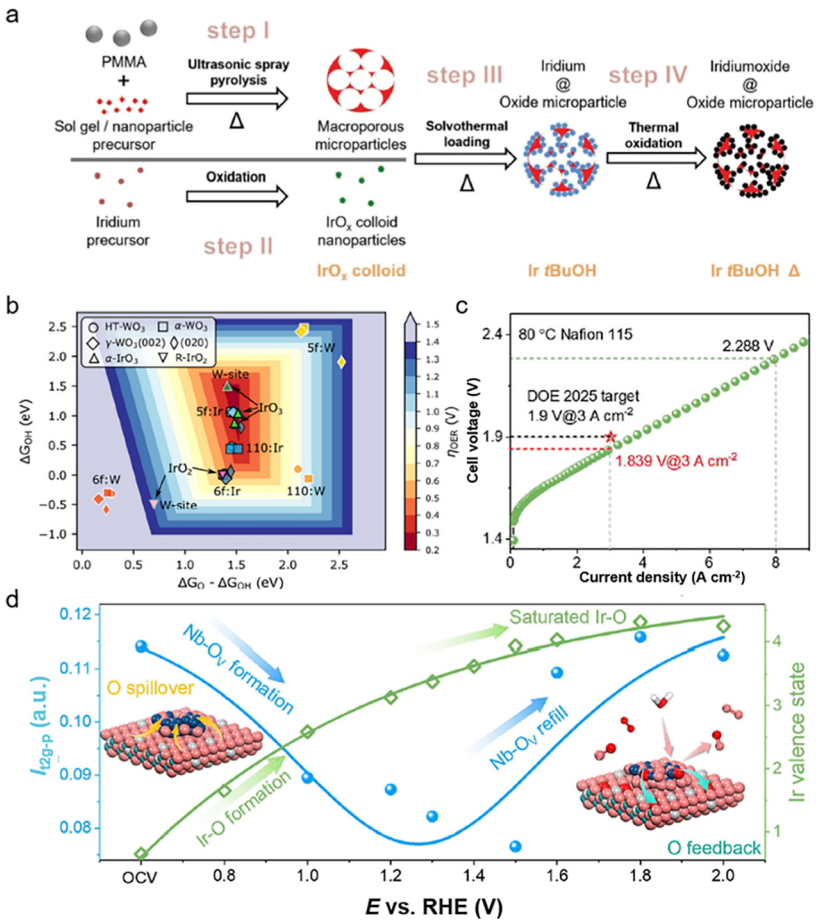

Fig. 5 (a) Synthesis of the ATO microparticle-supported IrO_2 oxygen evolution reaction catalyst (reproduced with permission from ref. 64, Copyright (2020) Wiley-VCH GmbH); (b) summary of the theoretical OER activities of various pure and doped HT (circles)-, α (squares)-, and γ-WO_3 (diamonds) surface models as well as selected α-IrO_3 (up triangles) and R-IrO_2 (down triangles) models (reproduced with permission from ref. 66, Copyright (2022) American Chemical Society); (c) polarization curve of the PEM electrolyzer obtained at 80 °C with a Nafion 115 membrane; (d) illustration of the overall dynamic interface effect (reproduced with permission from ref. 15, Copyright (2022) Wiley-VCH GmbH).

underwent dynamic migration of oxygen species between IrO_x and Nb_2O_{5-x} during the OER to suppress their over-oxidation, displayed high activity and stability in scalable water electroyzers. They only require 1.839 V to attain 3 A cm^{-2} (surpassing the DOE 2025 target) and demonstrate almost no decay during a 2000 h test at 2 A cm^{-2} (Fig. 5c and d). Therefore, the oxide support can indeed inhibit the degradation of the active center and tune the adsorption energy of oxygen intermediates on Ir-based catalysts through the metal–support interactions. The presence of supports may lead to the redistribution of charge in the catalyst, thus modifying its electronic structure.[67] Moreover, the dynamic migration of oxygen species or charge transfer may occur between the oxide support and Ir active sites. According to the previous reports, it may break the scaling relationship between the different oxygen species to achieve highly efficient OER performance. And it can also suppress the over-oxidation of Ir sites to achieve stable OER response.[15] At the same time, the stabilized oxides can also improve the vacancy formation energy of Ir in IrO_2, thus resulting in the enhancement of stability.[68,69]

4 Conclusions and perspectives

In conclusion, although Ir-based catalysts have exhibited relatively high OER performance, development of efficient Ir-based catalysts that meet the requirement of the working conditions for PEMWEs remains a major challenge. This review aims to focus on discussing the activation and degradation mechanism of Ir-based catalysts. And several modification strategies including elemental doping, surface engineering, atom utilization enhancing and support engineering for Ir-based catalysts are illustrated to uncover the mechanism. Table 1 summarizes the OER performance of the state-of-the-art Ir-based catalysts in PEMWEs. Even though achievements are obtained, studies on Ir-based catalysts should still be carried out to further realize their practical application.

Design of more effective OER catalysts

To date, the cost and OER performance of commercial Ir/C or IrO_2 still fall far short of the desired goals (*e.g.*, 2025 US DOE target, <1.9 V@3 A cm^{-2}). Therefore, it is necessary to

Table 1 Summary of the performance of representative Ir-based OER electrocatalysts in PEMWEs

OER catalyst	Overpotential in half-cell (@10 mA cm^{-2})	Activity in PEMWEs	Loading	Stability	Ref.
Ir/Nb_2O_{5-x}	218 mV	1.686 V@2.0 A cm^{-2}	1.8 mg_{Ir} cm^{-2}	2000 h	15
		2.123 V@6.0 A cm^{-2}		150 h	
GB-$Ta_xTm_yIr_{1-x-y}O_{2-\delta}$	198 mV	1.868 V@1.5 A cm^{-2}	0.8 mg_{Ir} cm^{-2}	500 h	47
Sr_2CaIrO_6	—	2.200 V@2.0 A cm^{-2}	0.2 mg_{Ir} cm^{-2}	1000 h	70
SrRuIr	190 mV	1.500 V@1.0 A cm^{-2}	1.5 mg_{Ir} cm^{-2}	150 h	71
Sr_2CaIrO_6	250 mV	1.810 V@2.0 A cm^{-2}	0.4 mg_{Ir} cm^{-2}	450 h	72
Ir/TiO_2–MoO_x	290 mV	1.740 V@1.0 A cm^{-2}	0.5 mg_{Ir} cm^{-2}	50 h	73
$Y_2Ru_{1.2}Ir_{0.8}O_7$	220 mV	1.645 V@0.1 A cm^{-2}	4.0 mg_{Ir} cm^{-2}	150 h	19
IrO_2/TNO-H750	—	1.832 V@1.0 A cm^{-2}	2.5 mg_{Ir} cm^{-2}	100 h	74
IrO_2@TiO_2	—	1.600 V@2.0 A cm^{-2}	0.5 mg_{Ir} cm^{-2}	160 h	75
Ir@WO_xNR	330 mV	1.625 V@0.5 A cm^{-2}	0.5 mg_{Ir} cm^{-2}	1030 h	76
IrO_x/Zr_2ON_2	255 mV	1.735 V@1.0 A cm^{-2}	0.4 mg_{Ir} cm^{-2}	50 h	77
IrRu@WO_3	245 mV	1.606 V@0.5 A cm^{-2}	0.2 mg_{Ir+Ru} cm^{-2}	500 h	78
$W_{0.7}Ir_{0.3}O_y$	278 mV	1.850 V@0.5 A cm^{-2}	0.4 mg_{Ir} cm^{-2}	500 h	79
Mn–RuIr NCT	198 mV	1.423 V@0.1 A cm^{-2}	1.0 mg_{Ir+Ru} cm^{-2}	10 h	80
IrO_x/W–TiO_2	—	1.602 V@1.0 A cm^{-2}	0.1 mg_{Ir} cm^{-2}	450 h	81
$IrO_x{\cdot}nH_2O$	300 mV	1.770 V@1.0 A cm^{-2}	3.0 mg_{Ir} cm^{-2}	600 h	82
CrO_2–0.16IrO_2	—	1.630 V@1.0 A cm^{-2}	0.6 mg_{Ir} cm^{-2}	100 h	83

rationally modulate the electronic structure and valence state of Ir-based catalysts according to the mechanisms involved. In general, the adsorption energy of oxygenated intermediate on pure IrO_2 is slightly higher than the optimal value. So, it is necessary to optimize the adsorption energy of the oxygen species by modulating the electronic structure of Ir sites (*e.g.*, lowering the d-band center of Ir active site) through elemental doping or surface engineering. Based on the activation and dissolution mechanism, obtaining highly active and stable Ir-based catalysts requires the avoidance of over-oxidation during the OER. And the preservation of the Ir valence state at the applied potential can be realized by tuning the dynamic migration of oxygen atoms through the Ir–support interaction. Further lowering the Ir loading may be an effective way to decrease the price of OER catalysts and expand their practical application. Atomization of Ir catalysts is a promising way to reduce the cost of the catalysts. Moreover, embedding Ir single atoms in some oxides with strong binding energy may help improve the catalysts' performance at high currents and voltages. In addition, the utilization of cheaper metal substitutes such as Ru and Fe may also reduce the cost, but the stability still needs to be improved. Therefore, the rational design of OER catalysts is still the key point for wider application of hydrogen production by water electrolysis.

Insightful mechanism investigation

Electrochemical catalysis is a dynamic process, while the active centers of catalysts undergo electron transport and valence change at high potential during the OER. To further understand the structure–performance relationship of the Ir-based catalysts, the morphology, electronic structure and density of states of the catalysts during the OER need to be described in detail by coupling *in situ* characterization and DFT calculations. Advanced characterization techniques, especially *in situ* X-ray absorption near edge structure spectroscopy, *in situ* Raman spectroscopy, *in situ* high-resolution transmission electron microscopy and *in situ* inductively coupled plasma mass spectrometry, are effective methods to obtain insight into Ir-based catalysts in the OER process. Thermodynamic calculations and kinetic simulations based on the rational model constructing can theoretically reveal some conclusions that can hardly be detected in experiments, such as the change of active sites. Therefore, more important information about the OER mechanism of the Ir-based catalysts can be obtained by combining the dynamic experimental data with the theoretical results.

Optimization of the contact interface at the PEMWE level

The performance of the catalyst in PEMWEs can be significantly affected by the mass transfer and interfacial resistance in the devices. As mentioned above, reducing the catalyst loading is an important way to reduce the costs. However, the performance of low loading Ir catalysts in PEMWEs would be relatively low due to the insufficient electron transport and mass transfer. Since PEMWEs need to achieve current densities above 1 A cm^{-2} and voltages of ~2 V, the various interface resistances of the device components need to be adjusted to reduce additional energy consumption and to achieve long-term stability under operating conditions. It is well known that the oxidation of the porous transport layer (PTL) is inevitable at high current and voltage. Due to the presence of excessive Schottky barrier, the electron transfer resistance between the oxidized PTL and the IrO_x catalytic layer (CL) will be greatly increased. Therefore, in order to reduce the interfacial resistance between PTL and CL, it is necessary to assemble devices using corrosion resistant PTLs with a similar Fermi energy level to IrO_x. The other interface components are ionomer/PTL and ionomer/CL. If the ionomers are too few, the mass transfer in the CL would be drastically reduced due to insufficient H^+. When the content of ionomers is too much and the loading of CL is

low, most of the ionomers would be in contact with the PTL, leading to a pinch-off effect and insufficient electron transport. Therefore, the addition of ionomers should be optimized and a moderate ionomer input would help improve the mass transfer and electron transport.

Conflicts of interest

The authors declare no conflict of interest.

Acknowledgements

This work was financially supported by the National Natural Science Foundation of China (22122202, 22072051, and 21972051).

References

1 Z. Fan and S. J. Friedmann, Low-carbon production of iron and steel: Technology options, economic assessment, and policy, *Joule*, 2021, **5**, 829–862.
2 X. Liu, S. Zhang, J. Liang, S. Li, H. Shi, J. Liu, T. Wang, J. Han and Q. Li, Protrusion-rich Cu@NiRu Core@shell nanotubes for efficient alkaline hydrogen evolution electrocatalysis, *Small*, 2022, **18**, e2202496.
3 Z. Lin, J. Liu, S. Li, J. Liang, X. Liu, L. Xie, G. Lu, J. Han, Y. Huang and Q. Li, Anti-corrosive SnS_2/SnO_2 heterostructured support for Pt nanoparticles enables remarkable oxygen reduction catalysis via interfacial enhancement, *Adv. Funct. Mater.*, 2023, **33**, 2211638.
4 C. V. Pham, D. Escalera-López, K. Mayrhofer, S. Cherevko and S. Thiele, Essentials of high performance water electrolyzers – From catalyst layer materials to electrode engineering, *Adv. Energy Mater.*, 2021, **11**, 2101998.
5 K. Zhang, X. Liang, L. Wang, K. Sun, Y. Wang, Z. Xie, Q. Wu, X. Bai, M. S. Hamdy, H. Chen and X. Zou, Status and perspectives of key materials for PEM electrolyzer, *Nano Res.*, 2022, **1**, e9120032.
6 Y. Chen, C. Liu, J. Xu, C. Xia, P. Wang, B. Y. Xia, Y. Yan and X. Wang, Key components and design strategy for a proton exchange membrane water electrolyzer, *Small Struct.*, 2022, 2200130.
7 A. Loncar, D. Escalera-Lopez, S. Cherevko and N. Hodnik, Inter-relationships between oxygen evolution and iridium dissolution mechanisms, *Angew. Chem., Int. Ed.*, 2022, **61**, e202114437.
8 A. S. Aricò, S. Siracusano, N. Briguglio, V. Baglio, A. Di Blasi and V. Antonucci, Polymer electrolyte membrane water electrolysis: Status of technologies and potential applications in combination with renewable power sources, *J. Appl. Electrochem.*, 2012, **43**, 107–118.
9 C. Fu, T. O'Carroll, S. Shen, L. Luo, J. Zhang, H. Xu and G. Wu, Metallic-Ir-based anode catalysts in PEM water electrolyzers: Achievements, challenges, and perspectives, *Curr. Opin. Electrochem.*, 2023, **38**, 101227.
10 F.-Y. Chen, Z.-Y. Wu, Z. Adler and H. Wang, Stability challenges of electrocatalytic oxygen evolution reaction: From mechanistic understanding to reactor design, *Joule*, 2021, **5**, 1704–1731.
11 Q. Wu, Y. Wang, K. Zhang, Z. Xie, K. Sun, W. An, X. Liang and X. Zou, Advances and status of anode catalysts for proton exchange membrane water electrolysis technology, *Mater. Chem. Front.*, 2023, **7**, 1025–1045.
12 A. R. Zeradjanin, J. Masa, I. Spanos and R. Schlögl, Activity and stability of oxides during oxygen evolution reaction—From mechanistic controversies toward relevant electrocatalytic descriptors, *Front. Energy Res.*, 2021, **8**, 613092.
13 M. Chatenet, B. G. Pollet, D. R. Dekel, F. Dionigi, J. Deseure, P. Millet, R. D. Braatz, M. Z. Bazant, M. Eikerling, I. Staffell, P. Balcombe, Y. Shao-Horn and H. Schafer, Water electrolysis: From textbook knowledge to the latest scientific strategies and industrial developments, *Chem. Soc. Rev.*, 2022, **51**, 4583–4762.
14 Z. Xu, L. Zhou, G. Zhou, S. Wu, P. Wang, H. Li, P. Huang and L. Liu, Light-driven Orderly Assembly of Ir-atomic Chains to Integrate a Dynamic Reaction Pathway for Acidic Oxygen Evolution, *Angew. Chem., Int. Ed.*, 2023, **62**, e2023011.
15 Z. Shi, J. Li, J. Jiang, Y. Wang, X. Wang, Y. Li, L. Yang, Y. Chu, J. Bai, J. Yang, J. Ni, Y. Wang, L. Zhang, Z. Jiang, C. Liu, J. Ge and W. Xing, Enhanced acidic water oxidation by dynamic migration of oxygen species at the Ir/Nb_2O_{5-x} catalyst/support interfaces, *Angew. Chem., Int. Ed.*, 2022, **61**, e202212341.
16 Z. Wang, X. Guo, J. Montoya and J. K. Nørskov, Predicting aqueous stability of solid with computed Pourbaix diagram using SCAN functional, *npj Comput. Mater.*, 2020, **6**, 160.
17 K. Zhang and R. Zou, Advanced transition metal-based oer electrocatalysts: Current Status, opportunities, and challenges, *Small*, 2021, **17**, e2100129.
18 L. Wang, L. Shi, Q. Liu, Y. Huang, W. Yan, X. Liang, X. Zhao, H. Chen and X. Zou, Structurally robust honeycomb layered strontium iridate as an oxygen evolution electrocatalyst in acid, *ACS Catal.*, 2023, **13**, 7322–7330.
19 H. Liu, Z. Zhang, M. Li, Z. Wang, X. Zhang, T. Li, Y. Li, S. Tian, Y. Kuang and X. Sun, Iridium doped pyrochlore ruthenates for efficient and durable electrocatalytic oxygen evolution in acidic media, *Small*, 2022, **18**, e2202513.
20 S. Hong, K. Ham, J. Hwang, S. Kang, M. H. Seo, Y. W. Choi, B. Han, J. Lee and K. Cho, Active motif change of Ni-Fe spinel oxide by Ir doping for highly durable and facile oxygen evolution reaction, *Adv. Funct. Mater.*, 2022, **33**, 2209543.
21 C. Wang, P. Zhai, M. Xia, Y. Wu, B. Zhang, Z. Li, L. Ran, J. Gao, X. Zhang, Z. Fan, L. Sun and J. Hou, Engineering lattice oxygen activation of iridium clusters stabilized on amorphous bimetal borides array for oxygen evolution reaction, *Angew. Chem., Int. Ed.*, 2021, **60**, 27126–27134.
22 X. Wang, H. Zhong, S. Xi, W. S. V. Lee and J. Xue, Understanding of oxygen redox in the oxygen evolution reaction, *Adv. Mater.*, 2022, **34**, e2107956.
23 Q. Wang, Y. Cheng, H. B. Tao, Y. Liu, X. Ma, D. S. Li, H. B. Yang and B. Liu, Long-term stability challenges and

opportunities in acidic oxygen evolution electrocatalysis, *Angew. Chem., Int. Ed.*, 2023, **62**, e202216645.

24 Z. Shi, Y. Wang, J. Li, X. Wang, Y. Wang, Y. Li, W. Xu, Z. Jiang, C. Liu, W. Xing and J. Ge, Confined Ir single sites with triggered lattice oxygen redox: Toward boosted and sustained water oxidation catalysis, *Joule*, 2021, **5**, 2164–2176.

25 M. Lu, Y. Zheng, Y. Hu, B. Huang, D. Ji, M. Sun, J. Li, Y. Peng, R. Si, P. Xi and C. H. Yan, Artificially steering electrocatalytic oxygen evolution reaction mechanism by regulating oxygen defect contents in perovskites, *Sci. Adv.*, 2022, **8**, eabq3563.

26 N. Zhang and Y. Chai, Lattice oxygen redox chemistry in solid-state electrocatalysts for water oxidation, *Energy Environ. Sci.*, 2021, **14**, 4647–4671.

27 H. Wu, Y. Wang, Z. Shi, X. Wang, J. Yang, M. Xiao, J. Ge, W. Xing and C. Liu, Recent developments of iridium-based catalysts for the oxygen evolution reaction in acidic water electrolysis, *J. Mater. Chem. A*, 2022, **10**, 13170–13189.

28 L. Gao, X. Cui, C. D. Sewell, J. Li and Z. Lin, Recent advances in activating surface reconstruction for the high-efficiency oxygen evolution reaction, *Chem. Soc. Rev.*, 2021, **50**, 8428–8469.

29 O. Kasian, J. P. Grote, S. Geiger, S. Cherevko and K. J. J. Mayrhofer, The common intermediates of oxygen evolution and dissolution reactions during water electrolysis on iridium, *Angew. Chem., Int. Ed.*, 2018, **57**, 2488–2491.

30 O. Kasian, J. P. Grote, S. Geiger, S. Cherevko and K. J. J. Mayrhofer, Die gemeinsamen Zwischenprodukte von Sauerstoffentwicklung und Auflösung während der Wasserelektrolyse an iridium, *Angew. Chem.*, 2018, **130**, 2514–2517.

31 S. Cherevko, S. Geiger, O. Kasian, A. Mingers and K. J. J. Mayrhofer, Oxygen evolution activity and stability of iridium in acidic media. Part 2. – Electrochemically grown hydrous iridium oxide, *J. Electroanal. Chem.*, 2016, **774**, 102–110.

32 H. Wang, Z. N. Chen, D. Wu, M. Cao, F. Sun, H. Zhang, H. You, W. Zhuang and R. Cao, Significantly enhanced overall water splitting performance by partial oxidation of Ir through au modification in core-shell alloy structure, *J. Am. Chem. Soc.*, 2021, **143**, 4639–4645.

33 Y. Wang, Y. Pang, H. Xu, A. Martinez and K. S. Chen, PEM Fuel cell and electrolysis cell technologies and hydrogen infrastructure development – A review, *Energy Environ. Sci.*, 2022, **15**, 2288–2328.

34 X. Liu, Z. Zhao, J. Liang, S. Li, G. Lu, C. Priest, T. Wang, J. Han, G. Wu, X. Wang, Y. Huang and Q. Li, Inducing covalent atomic interaction in intermetallic Pt alloy nanocatalysts for high-performance fuel cells, *Angew. Chem., Int. Ed.*, 2023, **62**, e202302134.

35 J. Liang, N. Li, Z. Zhao, L. Ma, X. Wang, S. Li, X. Liu, T. Wang, Y. Du, G. Lu, J. Han, Y. Huang, D. Su and Q. Li, Tungsten-doped l10 -ptco ultrasmall nanoparticles as a high-performance fuel cell cathode, *Angew. Chem., Int. Ed.*, 2019, **58**, 15471–15477.

36 J. Liang, X. Liu and Q. Li, Principles, strategies, and approaches for designing highly durable platinum-based catalysts for proton exchange membrane fuel cells, *Acta Phys.-Chim. Sin.*, 2020, **9**, 2010072-0.

37 T. Jian, W. Ma, C. Xu, H. Liu and J. Wang, Intermetallic-driven highly reversible electrocatalysis in Li–CO_2 battery over nanoporous Ni_3Al/Ni heterostructure, *eScience*, 2023, **3**, 100114.

38 J. Bai, L. Yang, Z. Jin, J. Ge and W. Xing, Advanced Pt-based intermetallic nanocrystals for the oxygen reduction reaction, *Chin. J. Catal.*, 2022, **43**, 1444–1458.

39 L.-W. Chen, F. He, R.-Y. Shao, Q.-Q. Yan, P. Yin, W.-J. Zeng, M. Zuo, L. He and H.-W. Liang, Intermetallic IrGa-IrO_x core-shell electrocatalysts for oxygen evolution, *Nano Res.*, 2021, **15**, 1853–1860.

40 P. Strasser, Free electrons to molecular bonds and back: closing the energetic oxygen reduction (ORR)-oxygen evolution (OER) cycle using core-shell nanoelectrocatalysts, *Acc. Chem. Res.*, 2016, **49**, 2658–2668.

41 Z. Wang, J. Huang, L. Wang, Y. Liu, W. Liu, S. Zhao and Z. Q. Liu, Cation-tuning induced d-band center modulation on Co-based spinel oxide for oxygen reduction/evolution reaction, *Angew. Chem., Int. Ed.*, 2022, **61**, e202114696.

42 H. Xu, J. Yang, R. Ge, J. Zhang, Y. Li, M. Zhu, L. Dai, S. Li and W. Li, Carbon-based bifunctional electrocatalysts for oxygen reduction and oxygen evolution reactions: Optimization strategies and mechanistic analysis, *J. Energy Chem.*, 2022, **71**, 234–265.

43 F. F. Zhang, C. Q. Cheng, J. Q. Wang, L. Shang, Y. Feng, Y. Zhang, J. Mao, Q. J. Guo, Y. M. Xie, C. K. Dong, Y. H. Cheng, H. Liu and X. W. Du, Iridium oxide modified with silver single atom for boosting oxygen evolution reaction in acidic media, *ACS Energy Lett.*, 2021, **6**, 1588–1595.

44 J. He, G. Fu, J. Zhang, P. Xu and J. Sun, Multistage electron distribution engineering of iridium oxide by codoping W and Sn for enhanced acidic water oxidation electrocatalysis, *Small*, 2022, **18**, e2203365.

45 X. Du, J. Huang, J. Zhang, Y. Yan, C. Wu, Y. Hu, C. Yan, T. Lei, W. Chen, C. Fan and J. Xiong, Modulating electronic structures of inorganic nanomaterials for efficient electrocatalytic water splitting, *Angew. Chem., Int. Ed.*, 2019, **58**, 4484–4502.

46 B. You, M. T. Tang, C. Tsai, F. Abild-Pedersen, X. Zheng and H. Li, Enhancing electrocatalytic water splitting by strain engineering, *Adv. Mater.*, 2019, **31**, e1807001.

47 S. Hao, H. Sheng, M. Liu, J. Huang, G. Zheng, F. Zhang, X. Liu, Z. Su, J. Hu, Y. Qian, L. Zhou, Y. He, B. Song, L. Lei, X. Zhang and S. Jin, Torsion strained iridium oxide for efficient acidic water oxidation in proton exchange membrane electrolyzers, *Nat. Nanotechnol.*, 2021, **16**, 1371–1377.

48 F. Liao, K. Yin, Y. Ji, W. Zhu, Z. Fan, Y. Li, J. Zhong, M. Shao, Z. Kang and Q. Shao, Iridium oxide nanoribbons with metastable monoclinic phase for highly efficient electrocatalytic oxygen evolution, *Nat. Commun.*, 2023, **14**, 1248.

49 H. Tang, Y. Su, B. Chi, J. Zhao, D. Dang, X. Tian, S. Liao and G.-R. Li, Nodal PtNi nanowires with Pt skin and controllable Near-Surface composition for enhanced oxygen reduction

electrocatalysis in fuel cells, *Chem. Eng. J.*, 2021, **418**, 129322.

50 M. Kim, J. Park, M. Wang, Q. Wang, M. J. Kim, J. Y. Kim, H.-S. Cho, C.-H. Kim, Z. Feng, B.-H. Kim and S. W. Lee, Role of surface steps in activation of surface oxygen sites on Ir nanocrystals for oxygen evolution reaction in acidic media, *Appl. Catal., B*, 2022, **302**, 120834.

51 C. Wang, A. Schechter and L. Feng, Iridium-based catalysts for oxygen evolution reaction in acidic media: Mechanism, catalytic promotion effects and recent progress, *Nano Research Energy*, 2023, **2**, e9120056.

52 X. Xi, J. Liu, H. Wu and W. Jiang, Highly crystalline nickel borate nanorods as oxygen evolution reaction electrocatalysts, *Journal of Electrochemistry*, 2018, **4**, 319–323.

53 S. Lee, Y. J. Lee, G. Lee and A. Soon, Activated chemical bonds in nanoporous and amorphous iridium oxides favor low overpotential for oxygen evolution reaction, *Nat. Commun.*, 2022, **13**, 3171.

54 N. Jing, Z. Shi, X. Wang, Y. Wang, H. Wu, C. Liu, J. Ge and W. Xing, Recent development of low iridium electrocatalysts toward efficient water oxidation, *Journal of Electrochemistry*, 2022, **9**, 2214010.

55 M. Malinovic, P. Paciok, E. S. Koh, M. Geuß, J. Choi, P. Pfeifer, J. P. Hofmann, D. Göhl, M. Heggen, S. Cherevko and M. Ledendecker, Size-controlled synthesis of IrO_2 nanoparticles at high temperatures for the oxygen evolution reaction, *Adv. Energy Mater.*, 2023, 2301450.

56 M. Xiao, J. Zhu, G. Li, N. Li, S. Li, Z. P. Cano, L. Ma, P. Cui, P. Xu, G. Jiang, H. Jin, S. Wang, T. Wu, J. Lu, A. Yu, D. Su and Z. Chen, A single-atom iridium heterogeneous catalyst in oxygen reduction reaction, *Angew. Chem., Int. Ed.*, 2019, **58**, 9640–9645.

57 Z. Lei, W. Cai, Y. Rao, K. Wang, Y. Jiang, Y. Liu, X. Jin, J. Li, Z. Lv, S. Jiao, W. Zhang, P. Yan, S. Zhang and R. Cao, Coordination modulation of iridium single-atom catalyst maximizing water oxidation activity, *Nat. Commun.*, 2022, **13**, 24.

58 J. Yin, J. Jin, M. Lu, B. Huang, H. Zhang, Y. Peng, P. Xi and C. H. Yan, Iridium single atoms coupling with oxygen vacancies boosts oxygen evolution reaction in acid media, *J. Am. Chem. Soc.*, 2020, **142**, 18378–18386.

59 X. Zhang, C. Yang, C. Gong, M. Liu, W. Zhou, H. Su, F. Yu, F. Hu, Q. Liu and S. Wei, Fast modulation of d-band holes quantity in the early reaction stages for boosting acidic oxygen evolution, *Angew. Chem., Int. Ed.*, 2023, e202308082.

60 Y. Wang, H. Su, Y. He, L. Li, S. Zhu, H. Shen, P. Xie, X. Fu, G. Zhou, C. Feng, D. Zhao, F. Xiao, X. Zhu, Y. Zeng, M. Shao, S. Chen, G. Wu, J. Zeng and C. Wang, Advanced electrocatalysts with single-metal-atom active sites, *Chem. Rev.*, 2020, **120**, 12217–12314.

61 L. Gao, X. Zhong, J. Chen, Y. Zhang, J. Liu and B. Zhang, Optimizing the electronic structure of Fe-doped Co_3O_4 supported Ru catalyst via metal-support interaction boosting oxygen evolution reaction and hydrogen evolution reaction, *Chin. Chem. Lett.*, 2022, **34**, 108085.

62 S. Wang, T. Shen, C. Yang, G. Luo and D. Wang, Engineering iridium-based oxygen evolution reaction electrocatalysts for proton exchange membrane water electrolyzers, *ACS Catal.*, 2023, **13**, 8670–8691.

63 C. Wang, L. Jin, H. Shang, H. Xu, Y. Shiraishi and Y. Du, Advances in engineering RuO_2 electrocatalysts towards oxygen evolution reaction, *Chin. Chem. Lett.*, 2021, **32**, 2108–2116.

64 D. Böhm, M. Beetz, M. Schuster, K. Peters, A. G. Hufnagel, M. Döblinger, B. Böller, T. Bein and D. Fattakhova-Rohlfing, Efficient oer catalyst with low ir volume density obtained by homogeneous deposition of iridium oxide nanoparticles on macroporous antimony-doped tin oxide support, *Adv. Funct. Mater.*, 2019, **30**, 1906670.

65 Y. Lou, J. Xu, Y. Zhang, C. Pan, Y. Dong and Y. Zhu, Metal-support interaction for heterogeneous catalysis: From nanoparticles to single atoms, *Mater. Today Nano*, 2020, **12**, 100093.

66 X. Shi, H.-J. Peng, T. J. P. Hersbach, Y. Jiang, Y. Zeng, J. Baek, K. T. Winther, D. Sokaras, X. Zheng and M. Bajdich, Efficient and stable acidic water oxidation enabled by low-concentration, high-valence iridium sites, *ACS Energy Lett.*, 2022, **7**, 2228–2235.

67 W. K. Han, J. X. Wei, K. Xiao, T. Ouyang, X. Peng, S. Zhao and Z. Q. Liu, Activating lattice oxygen in layered lithium oxides through cation vacancies for enhanced urea electrolysis, *Angew. Chem., Int. Ed.*, 2022, **61**, e202206050.

68 Z. Shi, J. Li, Y. Wang, S. Liu, J. Zhu, J. Yang, X. Wang, J. Ni, Z. Jiang, L. Zhang, Y. Wang, C. Liu, W. Xing and J. Ge, Customized reaction route for ruthenium oxide towards stabilized water oxidation in high-performance PEM electrolyzers, *Nat. Commun.*, 2023, **14**, 843.

69 S. Li, J. Liu, J. Liang, Z. Lin, X. Liu, Y. Chen, G. Lu, C. Wang, P. Wei, J. Han, Y. Huang, G. Wu and Q. Li, Tuning oxygen vacancy in SnO_2 inhibits Pt migration and agglomeration towards high-performing fuel cells, *Appl. Catal., B*, 2023, **320**, 122017.

70 J. Torrero, T. Morawietz, D. García Sanchez, D. Galyamin, M. Retuerto, V. Martin-Diaconescu, S. Rojas, J. A. Alonso, A. S. Gago and K. A. Friedrich, High performance and durable anode with 10-fold reduction of iridium loading for proton exchange membrane water electrolysis, *Adv. Energy Mater.*, 2023, 2204169.

71 Y. Wen, P. Chen, L. Wang, S. Li, Z. Wang, J. Abed, X. Mao, Y. Min, C. T. Dinh, P. Luna, R. Huang, L. Zhang, L. Wang, L. Wang, R. J. Nielsen, H. Li, T. Zhuang, C. Ke, O. Voznyy, Y. Hu, Y. Li, W. A. Goddard, III, B. Zhang, H. Peng and E. H. Sargent, Stabilizing highly active Ru sites by suppressing lattice oxygen participation in acidic water oxidation, *J. Am. Chem. Soc.*, 2021, **143**, 6482–6490.

72 M. Retuerto, L. Pascual, J. Torrero, M. A. Salam, A. Tolosana-Moranchel, D. Gianolio, P. Ferrer, P. Kayser, V. Wilke, S. Stiber, V. Celorrio, M. Mokthar, D. G. Sanchez, A. S. Gago, K. A. Friedrich, M. A. Pena, J. A. Alonso and S. Rojas, Highly active and stable OER electrocatalysts derived from Sr_2MIrO_6 for proton exchange membrane water electrolyzers, *Nat. Commun.*, 2022, **13**, 7935.

73 E.-J. Kim, J. Shin, J. Bak, S. J. Lee, K. h. Kim, D. Song, J. Roh, Y. Lee, H. Kim, K.-S. Lee and E. Cho, Stabilizing role of Mo in TiO_2-MoOx supported Ir catalyst toward oxygen evolution reaction, *Appl. Catal., B*, 2021, **280**, 119433.

74 H. Lv, S. Wang, C. Hao, W. Zhou, J. Li, M. Xue and C. Zhang, Oxygen-deficient $Ti_{0.9}Nb_{0.1}O_{2-x}$ as an efficient anodic catalyst support for PEM water electrolyzer, *ChemCatChem*, 2019, **11**, 2511–2519.

75 C. V. Pham, M. Bühler, J. Knöppel, M. Bierling, D. Seeberger, D. Escalera-López, K. J. J. Mayrhofer, S. Cherevko and S. Thiele, IrO_2 coated TiO_2 core-shell microparticles advance performance of low loading proton exchange membrane water electrolyzers, *Appl. Catal., B*, 2020, **269**, 118762.

76 G. Jiang, H. Yu, Y. Li, D. Yao, J. Chi, S. Sun and Z. Shao, Low-Loading and highly stable membrane electrode based on an Ir@WO_xNR ordered array for PEM water electrolysis, *ACS Appl. Mater. Interfaces*, 2021, **13**, 15073–15082.

77 C. Lee, K. Shin, Y. Park, Y. H. Yun, G. Doo, G. H. Jung, M. Kim, W. C. Cho, C. H. Kim, H. M. Lee, H. Y. Kim, S. Lee, G. Henkelman and H. S. Cho, Catalyst-support interactions in Zr_2ON_2-supported IrO_x electrocatalysts to break the trade-off relationship between the activity and stability in the acidic oxygen evolution reaction, *Adv. Funct. Mater.*, 2023, 2301557.

78 G. Jiang, H. Yu, D. Yao, Y. Li, J. Chi, H. Zhang and Z. Shao, Boosting the oxygen evolution stability and activity of a heterogeneous IrRu bimetallic coating on a WO_3 nano-array electrode for PEM water electrolysis, *J. Mater. Chem. A*, 2022, **10**, 11893–11903.

79 T. Yan, S. Chen, W. Sun, Y. Liu, L. Pan, C. Shi, X. Zhang, Z. F. Huang and J. J. Zou, IrO_2 nanoparticle-decorated Ir-doped $W_{18}O_{49}$ nanowires with high mass specific OER activity for proton exchange membrane electrolysis, *ACS Appl. Mater. Interfaces*, 2023, **15**, 6912–6922.

80 J. Joo, Y. Park, J. Kim, T. Kwon, M. Jun, D. Ahn, H. Baik, J. H. Jang, J. Y. Kim and K. Lee, Mn-dopant differentiating the Ru and Ir oxidation states in catalytic oxides toward durable oxygen evolution reaction in acidic electrolyte, *Small Methods*, 2022, **6**, e2101236.

81 X. Min, Y. Shi, Z. Lu, L. Shen, T. O. Ogundipe, P. Gupta, C. Wang, C. Guo, Z. Wang, H. Tan, S. Mukerjee and C. Yan, High performance and cost-effective supported IrO_x catalyst for proton exchange membrane water electrolysis, *Electrochim. Acta*, 2021, **385**, 138391.

82 J. Xu, H. Jin, T. Lu, J. Li, Y. Liu, K. Davey, Y. Zheng and S.-Z. Qiao, $IrO_x{\cdot}nH_2O$ with lattice water–assisted oxygen exchange for high-performance proton exchange membrane water electrolyzers, *Sci. Adv.*, 2023, **9**, eadh1718.

83 S. Ge, R. Xie, B. Huang, Z. Zhang, H. Liu, X. Kang, S. Hu, S. Li, Y. Luo, Q. Yu, J. Wang, G. Chai, L. Guan, H.-M. Cheng and B. Liu, A robust chromium–iridium oxide catalyst for high-current–density acidic oxygen evolution in proton exchange membrane electrolyzers, *Energy Environ. Sci.*, 2023, DOI: **10.1039/D3EE01192E**.